BIOCHEMISTRY
including biophysical chemistry & molecular biology

Article

pubs.acs.org/biochemistry

Conserved Hydrogen Bonding Networks of MitoNEET Tune Fe-S Cluster Binding and Structural Stability

Daniel W. Bak[†] and Sean J. Elliott*[,‡]

[†]Program in Molecular and Cellular Biology and Biochemistry and [‡]Department of Chemistry, Boston University, Boston, Massachusetts 02215, United States

Supporting Information

ABSTRACT: While its biological function remains unclear, the three-cysteine, one-histidine ligated human [2Fe-2S] cluster containing protein mitoNEET is of interest because of its interaction with the anti-diabetes drug pioglitazone. The mitoNEET [2Fe-2S] cluster demonstrates proton-coupled electron transfer (PCET) and marked cluster instability, which have both been linked to the single His ligand. Highly conserved hydrogen bonding networks, which include the His-87 ligand, exist around the [2Fe-2S] cluster. Through a series of site-directed mutations, PCET of the cluster has been examined, demonstrating that multiple sites of protonation exist in addition to the His ligand, which can influence redox potential. The mutations also demonstrate that while replacement of the His ligand with cysteine results in a stable cluster, the removal of Lys-55 also greatly stabilizes the cluster. We have also noted for the first time that the oxidation state of the cluster controls stability: the reduced cluster is stable, while the oxidized one is much more labile. Finally, it is shown that upon cluster loss the mitoNEET protein structure becomes less stable, while upon *in vitro* reconstitution, both the cluster and the secondary structure are recovered. Recently, two other proteins have been identified with a three-Cys(sulfur), one-His motif, IscR and Grx3/4-Fra2, both of which are sensors of iron and redox homeostatsis. These results lead to a model in which mitoNEET could sense the cellular oxidation state and proton concentration and respond through cluster loss and unfolding.

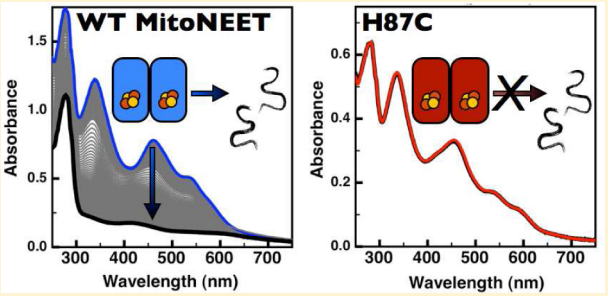

MitoNEET, a human [2Fe-2S] cluster binding protein,[1] was identified in 2004 as a binding target of pioglitazone,[2] a thiazolidinedione (TZD) family drug currently on the market to treat type II diabetes. MitoNEET is a small 12 kDa protein that exists as a dimer[1,3,4] (Figure 1A), tethered to the cytosolic face of the outer mitochondrial membrane (OMM) by an N-terminal helix.[1,5,6] Each protomer binds one [2Fe-2S] cluster, the first known OMM protein to do so. There is limited understanding of the role of this protein *in vivo*, though roles in iron−sulfur biogenesis,[7] iron trafficking,[8] redox signaling,[9] bioenergetics,[5,10] cell death and autophagy[11−13] have all been suggested.

The mitoNEET [2Fe-2S] cluster is uniquely ligated by three cysteine residues and a single histidine residue.[1] The mitoNEET family of proteins was the first known to have this type of cluster ligation, differing from the all-cysteine ligation of classical ferredoxins and the 2-His, 2-Cys ligation of Rieske clusters. It has been shown by our lab and others that several of the unusual properties that mitoNEET displays are the result of this unique histidine ligand.[14−17] The ε-nitrogen of the His ligand (His-87) may be protonated in the course of proton-coupled electron transfer (PCET) chemistry of the mitoNEET cluster. The same protonation also appears to confer pH-dependent instability to the Fe-S cluster. Replacement of His-87 with a cysteine ligand results in a bound cluster ligated by four cysteine ligands, but with drastically different PCET properties and greater stability.[14,15]

Interestingly, the His-87 ligand appears to be a part of a more extensive series of hydrogen bonding interactions within the mitoNEET dimer, illustrated by Figure 1. In particular, a lysine residue of the opposite protomer (Figure 1B,C), Lys-55, is conserved in higher eukaryotes, suggesting a conservation of this hydrogen bonding network. Additional H-bond interactions can be seen to exist between conserved residues Asp-84 and Ser-77, where Asp-84 appears to interact directly with one of the μ-sulfido ligands of the cluster (Figure 1B). Once again, these residues are absolutely conserved in mitoNEET homologues. Little attention has been given to the role of these conserved residues in PCET and cluster lability.

Here we have examined how His-87, Lys-55, Asp-84, and Ser-77 all contribute to the overall pH dependence of the midpoint potential and cluster loss. In both cases, it is clear that while the His-87 ligand is important, Lys-55 and to a lesser extent the Asp-84 and Ser-77 residues also play important roles in PCET and pH- and redox-induced cluster loss. We also report the first quantitative redox dependence of cluster loss, in

Received: April 30, 2013
Revised: June 11, 2013
Published: June 12, 2013

   dx.doi.org/10.1021/bi400540m | *Biochemistry* 2013, 52, 4687−4696

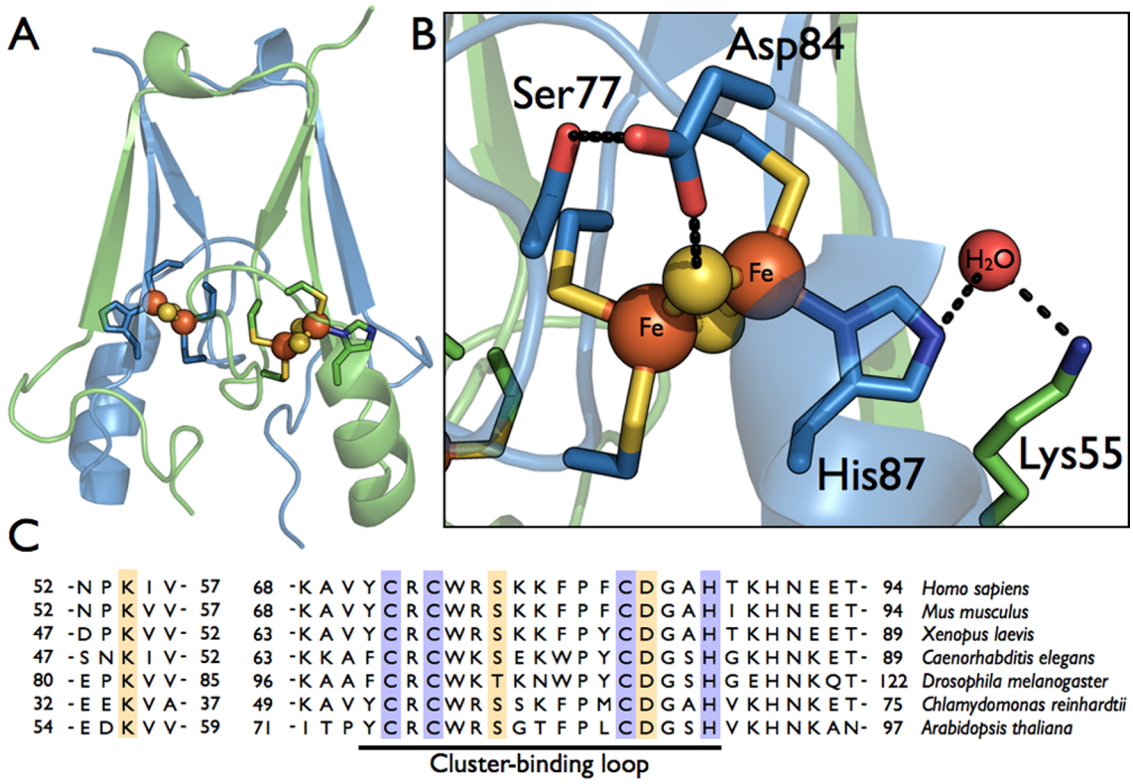

Figure 1. Structure and sequence comparison of human mitoNEET. (A) Dimeric mitoNEET protein displayed with each monomer (colored blue or green) containing one [2Fe-2S] cluster, ligated by three Cys ligands and a His ligand. (B) Cluster binding site, showing two hydrogen bonding networks, the first among the His-87 ligand, a conserved molecule of water, and Lys-55 and the second among a μ-sulfido ligand, Asp-84, and Ser-77. Proposed hydrogen bonds are represented by dashed lines. (C) Partial sequence alignment of various eukaryotic mitoNEET homologues. Conserved cluster ligands are highlighted in purple, and conserved residues involved in hydrogen bonding networks around the cluster are highlighted in gold. The cluster-binding loop is underlined.

which the oxidized cluster is significantly less stable than the reduced cluster. Additionally, we see pH-dependent protein structural instability as monitored by circular dichroism, which is strongly affected by replacement of the His ligand. These results help construct more detailed models of the interplay among mitoNEET protonation, cluster loss, and structural stability, which supports a protein function in either cluster transfer or redox sensing.

EXPERIMENTAL PROCEDURES

MitoNEET Construct and Mutagenesis. A truncated version of human mitoNEET, without the N-terminal 32-amino acid transmembrane helix, was codon-optimized for expression in *Escherichia coli* by Genscript (GenScript Corp., Piscatway, NJ). The gene was supplied in pUC57 with *Bam*HI and *Sal*I cloning sites. MitoNEET-pUC57 was digested with *Bam*HI and *Sal*I, and the mitoNEET insert was subcloned into pGEX-4T-3 (GE Healthcare), containing an N-terminal GST tag followed by a thrombin cleavage site (LVPRGS-). Correct ligation of the mitoNEET insert into the pGEX-4T-3 vector was confirmed by sequencing (GeneWiz).

The mitoNEET-pGEX-4T-3 plasmid was used as a template for generating four mitoNEET point mutants (H87C, K55I, D84N, and S77A) and two double mutants (H87C/K55I and H87C/D84N). Site-directed mutagenesis was performed using the QuikChange Lightning site-directed mutagenesis kit (Stratagene), with the following primers: replacement of His-87 with cysteine (H87C), 5′-C C G T T T T G C G A T G G C G C G T G T A C C A A A C A T A A C G A A G A A C-3′ and 5′-G T T T C T T C G T T A T G T T T G G T A C A C G C G C C A T C G C A A A A C G G-3′; replacement of Lys-55 with isoleucine (K55I), 5′-G C A T A T T C A G A A A G A T A A C C C G A T A A T T G T G C A T G C G T T T G A T A T G G-3′ and 5′-C C A T A T C A A A C G C A T G C A C A A T T A T C G G G T T A T C T T T C T G A A T A T G C-3′; replacement of Asp-84 with asparagine (D84N), 5′-C A A A A A A T T T C C G T T T T G C A A T G G C G C G C A T A C C A A A C-3′ and 5′-G T T T G G T A T G C G C G C C A T T G C A A A A C G G A A A T T T T T T G-3′; replacement of Ser-77 with alanine (S77A), 5′-G T A T T G C C G T T G C T G G C G T G C C A A A A A A T T T C C G T T T T G C G-3′ and 5′-C G C A A A A C G G A A A T T T T T T G G C A C G C C A G C A A C G G C A A T A C-3′. The double mutants were generated by a second round of site-directed mutagenesis on the H87C mitoNEET-pGEX-4T-3 plasmid using either the K55I primers or the following new H87C/D84N primers: 5′-C A A A A A A T T T C C G T T T T G C A A T G G C G C G T G T A C C A A A C-3′ and 5′-G T T T G G T A C A C G C G C C A T T G C A A A A C G G A A A T T T T T T G-3′. All mutations were confirmed via sequencing of the variant mitoNEET-pGEX-4T-3 construct (GeneWiz).

MitoNEET Overexpression and Purification. Recombinant wild-type mitoNEET and the mitoNEET variants were expressed from the pGEX-4T-3 (AmpR) vector in BL21(DE3) cells with the addition of 0.1 mM IPTG. Cells were grown aerobically overnight at room temperature in 2× YT medium with the addition of 1 g of ferrous ammonium sulfate/L of

dx.doi.org/10.1021/bi400540m | *Biochemistry* 2013, 52, 4687−4696

medium. Cells were harvested and purified in 1× PBS buffer (pH 8). Both PMSF and DNase I were added to the cell suspension. Lysis was accomplished with the addition of lysozyme and sonication, and after centrifugation at 15000*g*, the supernatant was retained. The lysate was loaded onto a glutathione-sepharose affinity resin, washed thoroughly, and incubated overnight in the presence of thrombin. The cleaved protein was eluted and, as a further purification step, run over a HiPrep 26/60 Sephacryl S-100 HR column attached to a refrigerated ÄKTApurifier FPLC system. Purity was confirmed by sodium dodecyl sulfate−polyacrylamide gel electrophoresis and Coomassie staining.

Protein Film Voltammetry. Electrochemical experiments were performed using a PGSTAT 12 AutoLab (Ecochemie) potentiostat, equipped with FRA and ECD modules. A three-electrode configuration was used, containing a platinum wire counter electrode and a saturated calomel reference electrode. Potentials were corrected by 242 mV to be reported versus the standard hydrogen electrode (SHE). Room-temperature cell solutions containing 0.1 M NaCl and 5 mM MES, MOPS, TAPS, CHES, and CAPS were used, with 5 mM sodium acetate added for the collection of H87C data. Pyrolytic graphite-edge (PGE) electrodes with a surface area of 1.4 mm^2 were used, and protein films were grown on electrodes by directly depositing 5 μL of ∼250 μM protein sample in 50 mM Tris and 100 mM NaCl (pH 8.5) (storage buffer) for approximately 5 min, followed by a rinse with distilled water to remove excess protein.

As previously reported with wild-type mitoNEET,[14] nonturnover electrochemical signals were generated on the benchtop with argon bubbled through the cell solution to remove excess oxygen. Data were collected at a scan rate of 100 mV/s between potentials of −0.9 and 0.1 V with a current range of 10 μA using the GPES software package (Ecochemie). Nonturnover signals were analyzed by subtraction of the baseline electrochemical response of the electrode surface from the raw data using the SOAS package.[18]

Proton-Coupled Electron Transfer Theory. Via variation of the pH of the buffer used in the electrochemical cell, the proton dependence of an electrochemical signal can be monitored. As the pH of the buffer solution is increased, the midpoint of the redox couple will shift to more negative values if the reduction potential is dependent on proton concentration (pH). This shift in reduction potential as a function of pH can be described by a variation of the Nernst equation[19] (eq 1).

$$E_{m,obs} = E_{acid} + \left(\frac{m}{n}\right)\left(\frac{RT}{F}\right) \times \ln\left(\frac{[H^+] + K_{red}}{[H^+] + K_{ox}}\right) \quad (1)$$

where the term m/n describes the ratio of the number of protons (m) and electrons (n) involved, K_{red} and K_{ox} are the equilibrium constants for the protonation of the reduced and oxidized species, respectively, and E_{acid} describes the reduction potential of the fully protonated species.

[2Fe-2S] Cluster Loss Assay. UV−visible absorption spectra were recorded in a 1 cm path length quartz cuvette at 25 °C on a Cary 50 Bio UV−visible spectrophotometer (Varian) equipped with a Cary single-cell Peltier accessory to control temperature. Full UV−visible spectra (200−800 nm) were recorded automatically at timed intervals. To initiate cluster loss, mitoNEET protein samples were diluted ∼10-fold into a 50 mM acetate, 100 mM NaCl buffer with low pH values (4−6) and quickly mixed. For the reduced protein, absolute anaerobic conditions were necessary to prevent reoxidation of the [2Fe-2S] cluster; therefore, the assay was performed in a sealed anaerobic quartz cuvette containing argon-sparged buffer supplemented with 5 mM ascorbate. The protein sample was prereduced with DTT (dithiothreitol) in an anaerobic glovebox and introduced into the assay using an airtight syringe. To account for the higher initial pH of the protein storage buffer, a final pH value was recorded for each reaction.

The half-life of cluster loss was determined at 336 nm by eq 2

$$A_{1/2(336)} = A_{i(336)} - [A_{i(336)} - A_{f(336)}]/2 \quad (2)$$

where $A_{i(336)}$ and $A_{f(336)}$ are the absorbance of the initial time point and the final time point, respectively, after the reaction had gone to completion. $t_{1/2}$ is the time point associated with $A_{1/2(336)}$. Data are reported as the average of three experiments, with the error reported in both the pH-based and time-based dimensions.

Generation of Apo-MitoNEET and Reconstituted MitoNEET. Generation of the apo form of mitoNEET by the removal of the [2Fe-2S] cluster could be accomplished by dilution of the protein sample into 50 mM sodium acetate and 100 mM NaCl (pH 4). The pH of the apoprotein sample was increased back to pH 8 for further characterization. Reconstitution of a [2Fe-2S] cluster into mitoNEET was accomplished through a modified *in vitro* assay[20] using the apo form of the protein as a target. DTT was added to a final concentration of 1 mM, followed by an addition of 100 μM ferrous ammonium sulfate and 100 μM sodium sulfide. The reaction was allowed to stand for 10 min, and then additional iron and sulfide (100 μM each) were added. This process was repeated once more so that the final concentration of iron and sulfide was 300 μM. The reaction mixture was allowed to sit for an additional 30 min before being loaded onto a PD10 desalting column, and the protein fractions were collected. The success of each individual reaction varied but would often return at minimum a 50% yield of reconstituted protein. This reconstituted mitoNEET was then used for further characterization.

Size-Exclusion Chromatography. Protein samples were run through a HiPrep 26/60 Sephacryl S-100 HR column, attached to a refrigerated ÄKTApurifier FPLC system. Samples were automatically injected onto the column after equilibration with phosphate buffer (pH 8). Samples were passed through the column in phosphate buffer (pH 8) at a flow rate of 1 mL/min. Protein elution was monitored by the ÄKTApurifier system at 280 nm.

Electron Paramagnetic Resonance. Low temperature (10 K) EPR measurements were made using a Bruker X-band EleXsys E-500 spectrometer equipped with an ESR900 continuous flow liquid helium cryostat. Reduced mitoNEET samples were generated by prior treatment with dithionite. EPR spectra were collected at 9.37 GHz, 2 mW microwave power, and with a 15 G modulation amplitude.

Circular Dichroism. Far-UV CD spectra (190−250 nm) were recorded at 20 °C on an Applied Photophysics CS/2 Chirascan circular dichroism spectrometer, equipped with a Peltier temperature controller unit. Using a 0.1 mm path length quartz cuvette, data were collected at 1 nm steps with an averaging time of 5 s/step. Protein concentrations of 250 μM in 25 mM sodium acetate, 25 mM sodium phosphate, and 50 mM sodium sulfate (pH adjusted with acetic acid) were used for data collection. Temperature melting curves were obtained with the same protein samples used for the far-UV CD measure-

dx.doi.org/10.1021/bi400540m | *Biochemistry* 2013, 52, 4687−4696

ments. The temperature was increased from 20 to 90 °C at a rate of 1 °C/min. Data were recorded at 200 and 470 nm every 1 °C with an averaging time of 5 s/step.

RESULTS

Production of MitoNEET Point Mutants. To interrogate the proton-dependent events of cluster reduction and cluster loss, four protonatable residues around the [2Fe-2S] cluster were targeted for site-directed mutations: His-87, Lys-55, Asp-84, and Ser-77. These positions contribute to two putative hydrogen bonding networks leading away from the [2Fe-2S] cluster (Figure 1B). A His−H_2O−Lys hydrogen bonding network is formed by the ε-nitrogen of the His ligand (His-87), a conserved water molecule, and the amine group of Lys-55, while a second S^{2-}−Asp−Ser network is formed by the more solvent-exposed cluster μ-sulfido ligand, the Asp-84 carboxylate, and the Ser-77 hydroxyl group. All site-directed mutations were introduced with the goal of eliminating the protonation site of the amino acid side chain, while otherwise being as conservative as possible [histidine to cysteine (H87C), lysine to isoleucine (K55I), aspartate to asparagine (D84N), and serine to alanine (S77A)].

For the sake of convenience, mitoNEET's N-terminal 32 amino acids were excluded from the recombinant construct generated for this work. As described for previous mitoNEET constructs, including the crystallographically characterized human[1,3,4] and *Arabidopsis*[21] proteins, omission of the N-terminal transmembrane helix resulted in no obvious deleterious effects on the soluble [2Fe-2S] cluster binding domain.[1,3,4] All four point mutants and the H87C/K55I and H87C/D84N double mutants could be readily expressed and easily solubilized. Reconstitution of the [2Fe-2S] cluster for further characterization was unnecessary as all mitoNEET variants fully incorporated their cluster when overexpressed in *E. coli*.

Proton-Coupled Electron Transfer at the MitoNEET [2Fe-2S] Cluster. Wild-type mitoNEET and site-directed variants were examined using direct electrochemistry with polished pyrolytic graphite edge (PGE) electrodes. For all variants, the voltammetric features were highly reversible: peak separations and widths at half-height are close to those predicted for a simple reversible one-electron process marked by facile interfacial electron transfer and a homogeneous protein monolayer (Figure 1 of Supporting Information).[22−24] A Pourbaix plot of reduction potential versus pH provides insight into the proton-dependent nature of the midpoint potential, reported here for mitoNEET and its variants (Figure 2).

We previously reported proton-dependent midpoint potentials for the wild-type protein,[14] which displayed an unexpectedly shallow gradient of only −40 mV per decade [Figure 2 (gray squares)]. This prevented the use of the Nernst equation for a single one-proton, one-electron couple, where the slope of the pH-dependent region is a −60 mV gradient. Instead, eq 3 was used to model a one-electron process coupled to two distinct protonation events.

$$E_{m,obs} = E_{alk} + \left(\frac{m}{n}\right)\left(\frac{RT}{F}\right) \times \ln\left(\frac{1 + \frac{[H^+]}{K_{red2}} + \frac{[H^+]^2}{K_{red1}K_{red2}}}{1 + \frac{[H^+]}{K_{ox2}} + \frac{[H^+]^2}{K_{ox1}K_{ox2}}}\right) \quad (3)$$

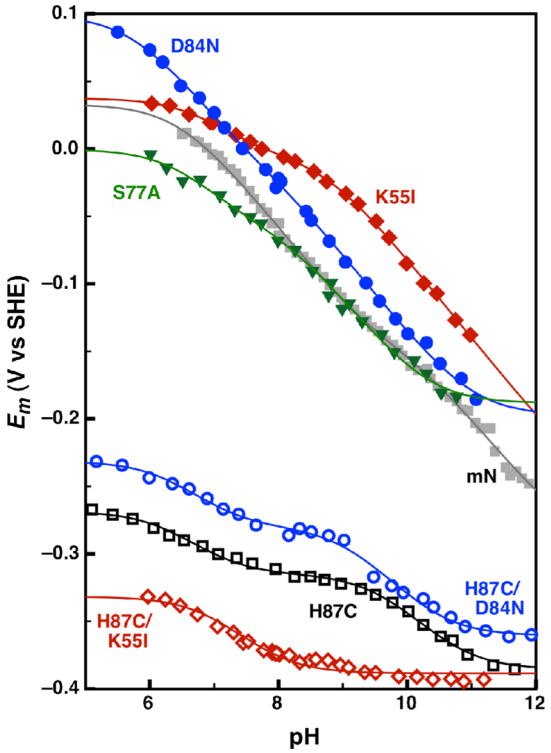

Figure 2. Comparison of the pH-dependent reduction potential for wild-type and site-directed variants of mitoNEET: wild type (solid squares), H87C (empty black squares), K55I (filled red diamonds), D84N (filled blue circles), S77A (filled green triangles), H87C/K55I (empty red diamonds), and H87C/D84N (empty blue circles). The wild-type, H87C, K55I, D84N, S77A, and H87C/D84N data were fit to a Nernst equation for four pK_a values (eq 3), while the H87C/K55I data were fit to a Nernst equation for two pK_a values (eq 1).

As in eq 1, the term m/n describes the ratio of the number of protons (m) and electrons (n) involved and E_{alk} describes the reduction potential of the fully deprotonated species. K_{red1} and K_{ox1} are the equilibrium constants of the reduced and oxidized species for the first protonation event, respectively, while K_{red2} and K_{ox2} are the equilibrium constants for the second protonation event. Unlike Rieske proteins, whose p$K_{ox1,2}$ and p$K_{red1,2}$ values are well separated, resulting in a −120 mV per decade region of two-proton one-electron coupling,[25,26] here the relative order of pK_a values differs (pK_{ox1} < pK_{red1} < pK_{ox2} < pK_{red2}), resulting in a shallower and more featured potential gradient for the mitoNEET [2Fe-2S] cluster. These two regions of pH dependence, between pK_{ox1} and pK_{red1} and between pK_{ox2} and pK_{red2}, will be termed neutral (6.5−9.5) and alkaline (10.0−12.5) regions of pH dependence, respectively. The strength of coupling can be established by ΔpK, the difference between pK_{red} and pK_{ox}. For reference, the His ligands in Reiske proteins display ΔpK values ranging from approximately 2 to 5.[26] Here we continue this analysis using a variety of site-directed mutants aimed at identifying the sites of protonation coupled to electron transfer. Table 1 lists and compares pK_a, ΔpK, and E_{acid} (the comparative midpoint potential of the fully protonated species) values for all mitoNEET mutants.

Mutation of the His-87 ligand or the Lys-55 residue significantly changes the pH dependence profiles in terms of the pK_a values and shifts in the midpoint potential of the mitoNEET cluster [Figure 2 (empty black squares and filled red diamonds)]. The pH dependence curves for both mutants

dx.doi.org/10.1021/bi400540m | *Biochemistry* 2013, 52, 4687−4696

Table 1. Reduction Potentials (E_{acid}) and pK_a Values for Wild-Type (WT) MitoNEET and Its Site-Directed Variants[a]

	E_{acid} (mV)	pK_{ox1}	pK_{red1}	ΔpK_1	pK_{ox2}	pK_{red2}	ΔpK_2
WT	14 ± 5	6.5 ± 0.1	9.5 ± 0.1	3.0	10.1 ± 0.1	12.6 ± 0.3[b]	2.5
H87C	−267 ± 1	6.3 ± 0.1	7.1 ± 0.1	0.8	9.64 ± 0.1	10.9 ± 0.1	1.2
K55I	37 ± 1	6.7 ± 0.1	7.5 ± 0.1	0.7	8.7 ± 0.1	13 ± 3[b]	4.3
S77A	−11 ± 4	6.4 ± 0.3[b]	7.4 ± 0.4[c]	1.0	8.1 ± 0.2[c]	10.3 ± 0.1	2.2
D84N	86 ± 5	5.7 ± 0.1	7.6 ± 0.3[c]	1.9	7.9 ± 0.3[c]	11.0 ± 0.1	3.1
H87C/D84N	−232 ± 2	6.3 ± 0.1	7.1 ± 0.1	0.8	9.1 ± 0.1	10.4 ± 0.1	1.4
H87C/K55I[d]	−331 ± 2	6.9 ± 0.1	7.9 ± 0.1	1.0			

[a]Unless otherwise indicated, the parameters are defined by eq 3. ΔpK is the difference between pK_{red} and pK_{ox}. Errors are calculated errors of the fitting process. [b]The lack of sufficient data at higher or lower ends of the pH range studied leads to larger uncertainties in pK_a. [c]Larger errors caused by an inability to properly define turning points when pK_{red1} and pK_{ox2} are similar. [d]Parameters are defined for this variant by eq 1.

share a weakly coupled neutral region of pH dependence with an approximate ΔpK of 1. Additionally, both mutants contain a more alkaline region of pH dependence, which is lost in the H87C/K55I double mutant [Figure 2 (empty red diamonds)]. This indicates that the weakly coupled alkaline pH dependence of the H87C mutant is likely due to the protonation of Lys-55, while the strongly coupled region of pH dependence in the K55I mutant is the result of His-87 protonation. This alkaline region of pH dependence in the K55I mutant with a pK_{ox} of 8.71 and a ΔpK of 4.3 is similar to the pH dependence profile of His ligands in Rieske proteins.[26]

The H87C/D84N double mutant was used [Figure 2 (empty blue circles)] to test whether the Asp-84 residue could be responsible for the neutral region of pH dependence seen for the previous mutants. Its pH dependence profile was similar to the profile of the H87C mutant, indicating that the Asp-84 residue likely is not responsible for the neutral region of pH dependence. The D84N and S77A mutants show minimal deviations from the wild-type pH dependence data [Figure 2 (filled blue circles and filled green triangles)], though small changes can be seen for both of these mutations. Specifically, the S77A mutation seems to affect the neutral region of pH dependence more strongly than the alkaline one.

These results confirm our earlier model in which the pH dependence of mitoNEET is not a simple one-proton, one-electron couple as suggested by others, where an empirical factor was used to fit the pH dependence.[27] As shown here, the interdependence of the hydrogen bond networks makes it difficult to assign the two regions of pH dependence in the wild-type protein, as any change made to the protein by the mutation of residues leads to a shift in the pK_a of the remaining residues.

Proton- and Redox-Dependent Loss of the MitoNEET [2Fe-2S] Cluster. The [2Fe-2S] cluster of wild-type mitoNEET has previously been shown to be unstable below neutral pH, while the H87C mutant has been shown to be resistant to pH-dependent cluster loss.[15] Because the His-87 ligand is not the sole determinant of the pH dependence of the midpoint potential, the additional point mutants (K55I, D84N, and S77A) were examined to identify their effect on the pH dependence of mitoNEET cluster loss. The dependence of cluster loss on redox state has also been examined here. Monitoring the presence of the MitoNEET [2Fe-2S] cluster by optical spectroscopy, we have confirmed reports of the instability of the oxidized wild-type protein at pH 5.20 (Figure 3A). The visible signal intensity (associated with the Fe−cysteinate ligand charge transfer[28]) had decayed to ~50% after 20 min, and almost fully within 1 h. In contrast, the reduced state of mitoNEET at pH 5.20 is almost completely stable

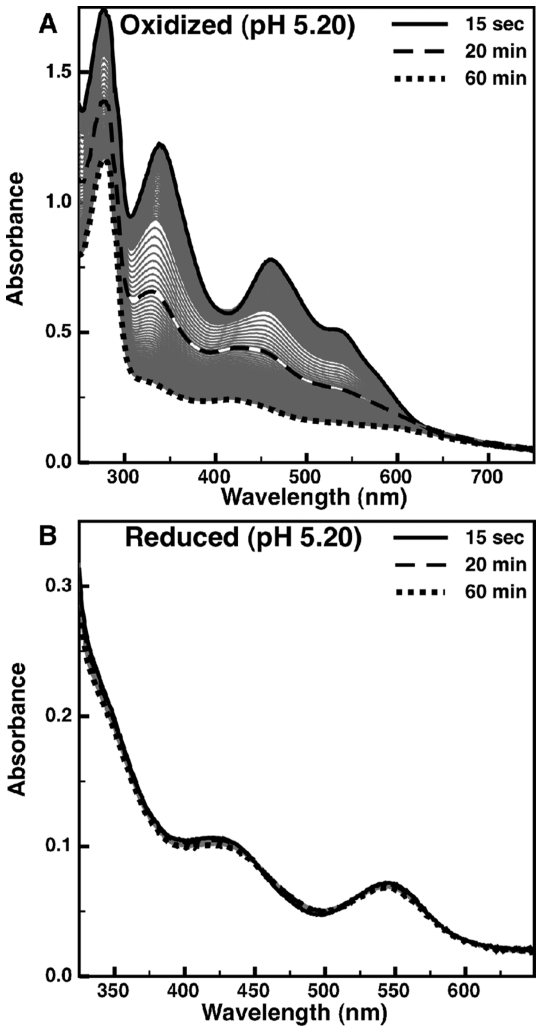

Figure 3. Time-dependent loss of visible absorption signals for mitoNEET at pH 5.20: (A) oxidized mitoNEET and (B) reduced mitoNEET. Time points of 15 s (solid), 20 min (dashed), and 90 min (dotted) are shown in bold, while intermediate time points are shown as thin gray traces.

(Figure 3B), with an only slight loss in the magnitude of the absorption signal after 1 h.

The cluster loss at pH 5.20−5.30 is shown for the wild-type protein and all four point mutants (Figure 4), with the exception of the H87C mutant, which is presented at pH 4.55. The H87C mutant is completely stable over the range of pH values assayed, demonstrating that His-87 is necessary for [2Fe-2S] cluster instability. Using the half-life of the optical signals as

dx.doi.org/10.1021/bi400540m | Biochemistry 2013, 52, 4687−4696

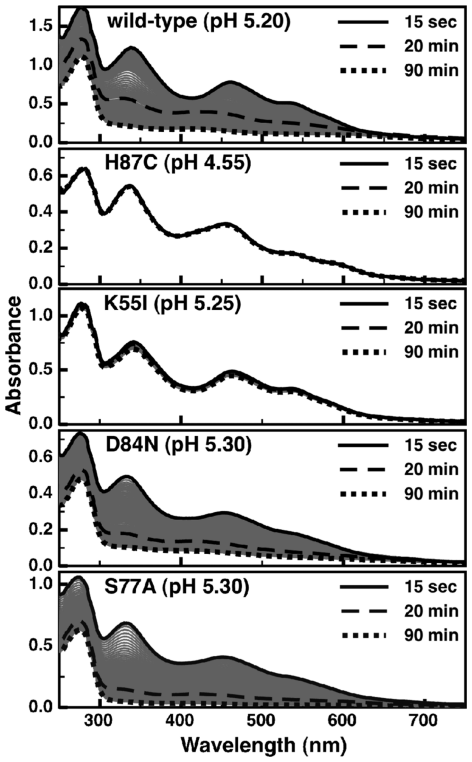

Figure 4. Time-dependent loss of visible absorption signals for wild-type mitoNEET and its site-directed variants: wild type at pH 5.20, H87C at pH 4.55, K55I at pH 5.25, D84N at pH 5.30, and S77A at pH 5.30. Time-points of 15 s (solid), 20 min (dashed), and 90 min (dotted) are shown in bold, with intermediate time points shown as thin gray traces.

a metric for the stability of the [2Fe-2S] cluster illustrates the variation of cluster stability as a function of pH (Figure 5). For example, the K55I mutant has a stabilizing effect on the [2Fe-2S] cluster at pH 5.25 (Figure 4), and it is also clear that removal of the amine group stabilizes the cluster significantly over a range of pH values, as evidenced by a shift of the cluster half-life curve [Figure 5 (black diamonds)]. Alternatively, both

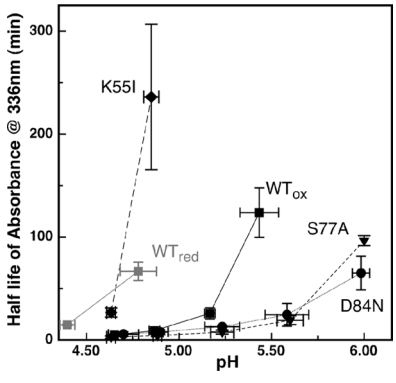

Figure 5. Comparison of the stability of the [2Fe-2S] cluster optical signals as a function of pH for wild-type mitoNEET and its site-directed variants: wild-type mitoNEET oxidized (black squares) and reduced (gray squares), K55I oxidized (black diemonds), D84N oxidized (black circles), and S77A oxidized (black upside down triangles). Oxidized H87C is not shown because of its complete stability in this pH range. Plotted is the half-life of the optical signal at 336 nm vs pH. Data points and error bars represent the average of three experiments.

the D84N and S77A mutants at pH 5.30 (Figure 4) and over a range of pH values [Figure 5 (black circles and black upside down triangles)] are less stable than the wild-type protein. This would suggest that the hydrogen bonding network created by these two residues and the μ-sulfido ligand has a stabilizing role to play with respect to the cluster.

***In Vitro* Reconstitution of Apo-MitoNEET.** To determine, at least *in vitro*, whether cluster loss is a reversible phenomenon, a reconstitution of apo-mitoNEET was performed under anaerobic conditions in an anaerobic glovebox. It was found that using DTT as an electron donor instead of dithionite and gradually adding small aliquots of Fe^{2+} and S^{2-} resulted in better yields of the reconstituted protein, as reported previously for human ferredoxin.[20] Reconstitution of the native [2Fe-2S] cluster was confirmed spectroscopically. The visible absorption bands associated with both the oxidized (Figure 6A)

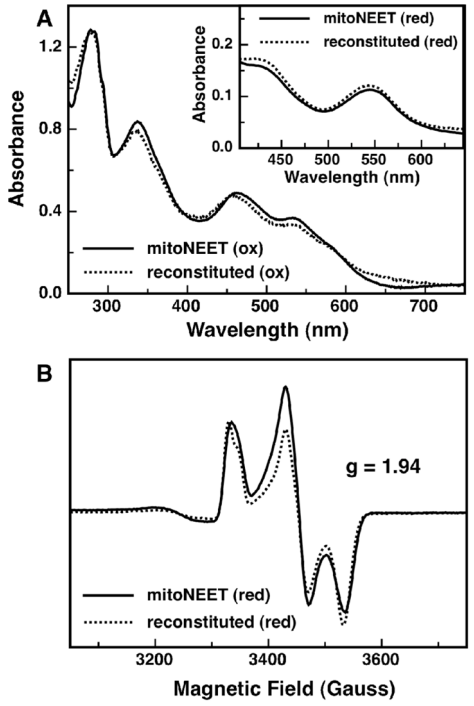

Figure 6. Spectroscopic characterization of reconstituted mitoNEET. (A) Optical spectra of oxidized reconstituted mitoNEET (dotted line) and as-isolated mitoNEET (solid line). The inset shows optical spectra of dithionite-reduced reconstituted mitoNEET (dotted line) and as-isolated mitoNEET (solid line). (B) Low-temperature (10 K) EPR spectra of dithionite-reduced reconstituted mitoNEET (dotted line) and as-isolated mitoNEET (solid line) measured at 9.24 GHz.

and reduced (Figure 6A, inset) states of the reconstituted protein match up well with those of the native form of the protein. Small deviations from the native absorption spectrum are most likely the result of some nonspecific Fe-S binding, but these appear to represent only a minor fraction of the overall sample. Reconstitution of the native cluster was also confirmed with electron paramagnetic resonance (EPR) (Figure 6B). EPR spectra for the reconstituted protein in the reduced state overlays nicely with that of the reduced native protein, both having *g* values of 1.94. Oxidized, reconstituted mitoNEET is EPR silent [like native protein (data not shown)]. It is clear that upon *in vitro* reconstitution, mitoNEET is capable of binding a [2Fe-2S] cluster with the same three-Cys, one-His

dx.doi.org/10.1021/bi400540m | *Biochemistry* 2013, 52, 4687−4696

ligand set as the native protein, suggesting that cluster loss is in theory a reversible event.

Structural Instability of Apo-MitoNEET. A significant decrease in the absorbance at 280 nm can be seen upon cluster loss for wild-type mitoNEET and its site-directed variants (Figure 4). The magnitude of the 280 nm signal is reduced by approximately one-third in the apo form of the protein as compared to that of the holo form. Each mitoNEET monomer contains one tryptophan residue (Trp-75), which is responsible for the majority of the protein-based UV absorbance around 280 nm. This tryptophan sits at the dimer interface and is buried from solvent exposure. As the optical absorbance of tryptophan can be affected by the local environment, upon loss of cluster, mitoNEET likely undergoes a conformational change that alters the local environment of the tryptophan residue.[29] Here, we have examined the impact of cluster loss upon the solution structure of mitoNEET in terms of both the quaternary structure of the mitoNEET dimer and the secondary structure of the protein.

To test whether mitoNEET was undergoing an oligomeric change upon cluster loss, both apo- and holo-mitoNEET were run on an S-100 size-exclusion column. Holo-mitoNEET eluted as only one major species around 20 kDa [Figure 7 (solid line)], representative of the dimeric protein. The apoprotein, after being generated at low pH, eluted as a mixture of higher-molecular mass species [Figure 7 (dotted line)]. Virtually no dimeric mitoNEET remained, and there was no indication of the monomeric species, suggesting multimerization and/or nonspecific aggregation occurs upon cluster loss.

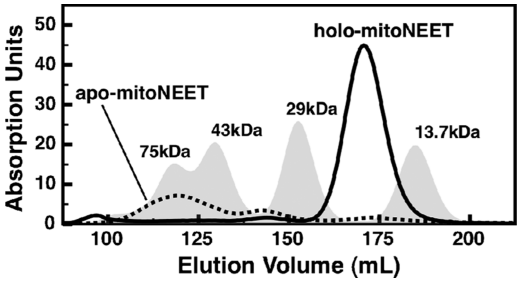

Figure 7. Size-exclusion chromatograms for wild-type mitoNEET: holo-mitoNEET (solid line) and apo-mitoNEET (dotted line). A set of four protein standards is reported for comparison (gray peaks): ribonuclease A (13.7 kDa), carbonic anhydrase (29 kDa), ovalbumin (43 kDa), and conalbumin (75 kDa). All chromatograms are calculated from the absorbance at 280 nm.

The far-UV CD spectra of oxidized mitoNEET display a negative feature centered at 220 nm (Figure 2 of the Supporting Information) and are suggestive of both α-helical and β-sheet content,[30] as would be anticipated for mitoNEET, which contains one three-strand β-sheet and two short α-helices per monomer. When mitoNEET is denatured by being heated to 90 °C, the magnitude of the negative feature at 220 nm diminishes and overall the negative features between 200 and 230 nm are broadened (Figure 2 of the Supporting Information). This spectrum is suggestive of a molten globule state that has been seen previously for unloaded iron−sulfur proteins.[31] Interestingly, this state can also be achieved by generating the apo form of the protein at low pH and 20 °C (Figure 2 of the Supporting Information), suggesting that the pH-dependent loss of cluster is concomitant with protein structure destabilization. Here pH appears to be a switch for protein unfolding that is as strong as heat denaturation is.

To improve our understanding of the effect of pH on protein stability, a series of temperature melts were performed with the wild-type, oxidized protein. Additionally, the CD characteristics in the visible region that are due to the presence of the oxidized cluster can similarly monitored at 470 nm (Figure 3 of the Supporting Information). In Figure 8, the depletion of secondary structure (monitored at 220 nm) and the presence of the Fe-S cluster (monitored at 470 nm) are shown as a function of temperature. At pH 8 [Figure 8 (bottom, filled black squares)], mitoNEET has an apparent melting temperature ($T_{m,app}$) of 75 °C (as this protein unfolding event is not reversible, true thermodynamic parameters cannot be determined). When unfolding measurements were repeated for mitoNEET at pH 7 and 6 [Figure 8 (bottom, half-filled and empty squares, respectively)], a significant shift was seen in the values of $T_{m,app}$, lowered to 65 °C for pH 7 and 50 °C for pH 6. The H87C mutant had a $T_{m,app}$ of 70 °C at pH 6 [Figure 8 (bottom panel, empty red diamonds)], indicating a significant increase in protein stability for this mutant. At higher pH values, the unfolding of the H87C mutant had not gone to completion by 90 °C, suggesting a $T_{m,app}$ of >90 °C.

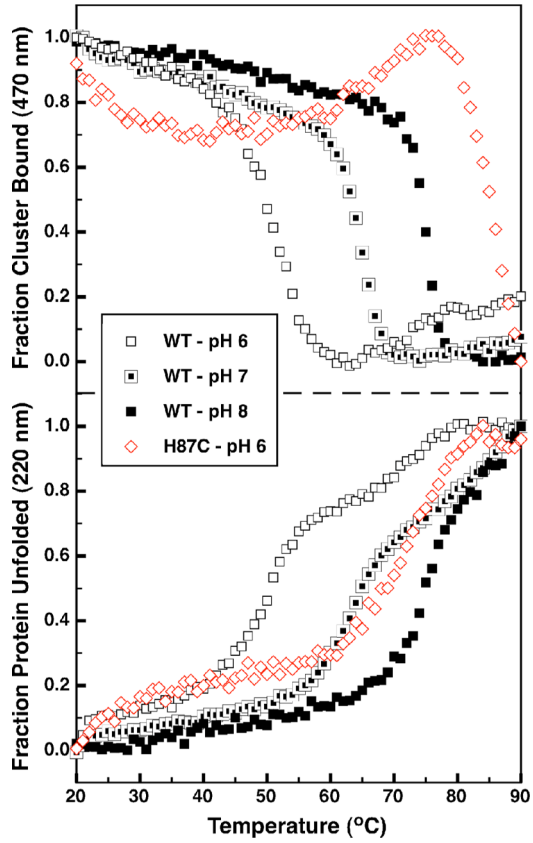

Figure 8. CD melting curves of wild-type mitoNEET and its H87C variant. The fraction of bound cluster as monitored by the 470 nm CD band (top) and the fraction of unfolded protein (bottom) for WT mitoNEET at pH 6 (empty black squares), pH 7 (half-filled black squares), and pH 8 (filled black squares) and for the H87C mutant at pH 6 (empty red diamonds).

Interestingly, for the wild-type protein, loss of the 470 nm signal (Figure 8, top) occurs at approximately the same temperature as $T_{m,app}$ at all pH values. This suggests a strong

dx.doi.org/10.1021/bi400540m | Biochemistry 2013, 52, 4687−4696

coupling between the loss of cluster and protein unfolding in mitoNEET. Alternatively, the loss of cluster in the H87C variant occurs at temperatures significantly higher than its $T_{m,app}$, suggesting that even in the unfolded state the four cysteine ligands of the H87C mutant are still ligating the Fe-S cluster, and at higher pH values, cluster loss in H87C had not fully occurred by 90 °C.

DISCUSSION

A clear picture of the role of mitoNEET has failed to emerge since the identification of this unique [2Fe-2S] cluster binding protein almost 10 years ago. It is presumed that at the heart of whatever biological function mitoNEET may have, the conservation of the cluster's lone ligating histidine (His-87) indicates a crucial role for this residue. Postulated roles in cluster transfer, bioenergetics, and redox sensing have all been put forth as possible functions for mitoNEET, where His-87 may be involved in tuning reduction potential,[27] controlling cluster stability,[15] and mitigating PCET.[14,27]

Little attention has been given to the fact that other highly conserved non-ligating residues exist around the cluster and participate in conserved hydrogen bonding networks. Lys-55 forms a hydrogen bonding network with His-87 through a conserved water molecule (present in all eukaryotic mitoNEET-like protein crystal structures[1,3,4,21,32]). This residue, donated from the opposite monomer, crosses the dimer interface, though in some bacterial/archaeal mitoNEET homologues this residue is at position $n + 1$ with respect to the His ligand, but still within hydrogen bonding distance of the histidine ε-nitrogen.[33] A second conserved hydrogen bond network (among Ser-77, Asp-84, and the more solvent-exposed cluster μ-sulfido ligand) is also conserved in all mitoNEET-like structures, with these residues also conserved in all mitoNEET-like sequences. Here, we have elucidated the role of these conserved residues and the effect of their hydrogen bonding networks on PCET and the stability of the mitoNEET [2Fe-2S] cluster.

The pH dependence curves for the multiple mitoNEET variants clearly show the importance of the PCET event associated with His-87, but unlike Rieske proteins where the ε-nitrogens of both His ligands are solvent-exposed,[34] here the His−H_2O−Lys network appears to act as a means of proton coupling to extend from the ligating residue to additional elements of protein structure. It is difficult to assign specific sites of protonation to each region of pH dependence because, for example, mutation of Lys-55 results in a shift in the pK_a values associated with the His-87 ligand. Most likely, the more alkaline pH dependence represents a protonation of the His−H_2O−Lys network, while the more neutral region of pH dependence might come from an alternative site. Additional hydrogen bonding networks in the interior of the protein and at the dimer interface, including Arg-73 and His-58, may also be involved in long-range PCET. In the case of some clusters, direct protonation at a μ-sulfido ligand is possible, as described for the [3Fe-4S] cluster of *Azotobacter vinelandii* ferredoxin I (AvFdI).[35]

Despite our inability to definitively assign the neutral PCET event, it is possible that it may be responsible for cluster lability, as the cluster becomes highly unstable below neutral pH. Cluster loss is additionally dependent on redox state, indicating a possible role in redox sensing. At physiological pH, the cytosolic resting potentials are approximately −290 mV,[36] suggesting that mitoNEET ($E_{m,7}$ = 0 mV) would primarily exist in a reduced state, which would be stable to cluster loss. Under oxidative stress conditions or certain physiological conditions such as apoptosis and differentiation,[37] where the cytosolic potential could rise as high as 200 mV, the cluster would become oxidized and susceptible to cluster loss.

As indicated by the more stable cluster half-lives of the H87C and K55I mutants, the His−H_2O−Lys hydrogen bonding network plays a significant role in cluster lability. While an argument could be made that cluster instability is tolerated because of the significant increase in midpoint potential afforded by the presence of His-87, the same argument does not hold for the Lys-55 residue. At neutral pH, loss of Lys-55 results in almost no change in redox potential. Thus, the highly conserved nature of this residue suggests that the mitoNEET protein may have evolved this hydrogen bonding network, not to tune reduction potential but to tune cluster stability. Indeed, protonation of His-87 is likely not a sole determinant of stability: Rieske centers, with two His ligands, but lacking the unique His−H_2O−Lys network, have never been shown to contain unstable clusters upon protonation of their ligands.[38] Together, these observations support the hypothesis that cluster transfer (or loss) due to redox sensing is of potential biological significance, as suggested previously.[7]

Here we have demonstrated that the quaternary and secondary structure of MitoNEET itself is intimately tied to whether the Fe-S cluster is bound. It has been noted previously that apo-ferredoxins adopt a molten globule-like state in the absence of their Fe-S clusters. For example, the [3Fe-4S][4Fe-4S] ferredoxin from *Acidianus ambivalens* (AaFd)[31] retains elements of secondary structure, and its compactness is like that of the holo-protein. Additionally, the IscU Fe-S scaffold proteins from *E. coli*[39−41] and *Thermotoga maritima*,[42−44] which only transiently host an Fe-S cluster, exist in equilibria between a more structured state and a disordered state in the absence of a cluster, yet the apparent lability of the MitoNEET Fe-S cluster may not entirely indicate a role in cluster transfer. The CD spectra of both the thermally unfolded and pH-unfolded state of mitoNEET are not suggestive of proteins with a random coil structure, suggesting that a degree of secondary structure remains. Additionally, the $T_{m,app}$ of both unfolding and cluster loss in the mitoNEET protein at neutral pH is much more comparable to those calculated for ferredoxin proteins (between 60 and 80 °C). For IscU-like proteins, the temperature associated with cluster loss is approximately 40 °C.[43] Interestingly, at lower pH values, the unfolding and cluster loss of mitoNEET more closely matches what is seen in IscU-like proteins. This could suggest that while the mitoNEET [2Fe-2S] cluster is not as transient as those seen in IscU-type proteins, under certain conditions the structural flexibility of the protein could enhance cluster transfer.

The mitoNEET homologue miner1 has been shown to interact with Beclin1/Bcl-2 at the ER−cytosol interface to inhibit signaling for autophagy but is incapable of protein interactions in the absence of the cluster.[11,13] This observation is easily explained if apo-miner1 is as structurally flexible as mitoNEET. This would be an intriguing and unique mechanism for signaling within cells; disruption of Fe-S cluster binding leading to a less structurally stable protein results in a loss of protein−protein interactions leading to downstream signaling effects. While the native protein partners of mitoNEET are unknown, it will be interesting to determine the conditions under which mitoNEET may be able to interact with them.

Recently, two other proteins have been identified with putative three-sulfur (Cys, glutathione), one-His ligand sets, where cluster lability is potentially significant to function: the bacterial transcription factor IscR[45] and the iron regulatory proteins Grx3/4 and Fra2 in yeast[46] and Glrx3 and BolA2 in humans.[47] *E. coli* IscR plays a role in Fe-S biogenesis as a sensor of the need for Fe-S cluster production.[48] In yeast, cytosolic monothiol glutaredoxins (Grx3 and Grx4) interact with Fra2 to form a [2Fe-2S] cluster at the dimer interface, which prevents activation of the Atf1/2 transcription factor and transcription of the iron regulon.[49] This interaction appears to be conserved in mammals, with Glrx3 and BolA2 interacting in a similar manner. Interestingly, IscR and Grx3/4-Fra2 both play a role in sensing the need for iron within the cell, and cluster loss likely prevents interactions with either DNA or proteins. The fact that these proteins, along with mitoNEET, possibly each ligate a [2Fe-2S] cluster with a single His ligand suggests that perhaps this ligation motif represents a functional strategy for sensing iron and redox homeostasis within a cell; however, the redox-dependent properties of these novel Cys/His ligated Fe-S clusters have been largely unexplored.

CONCLUSION

This study demonstrates that mitoNEET responds to both a decreased pH and an increased level of oxidative stress with the loss of its [2Fe-2S] cluster. This cluster loss is concomitant with loss of structural stability, but cluster assembly and protein refolding are facile. We believe this work will potentially direct future biological studies of the functional role of mitoNEET, whether that be redox sensing, cluster transfer, or some unknown role.

ASSOCIATED CONTENT

Supporting Information

Raw PFV data and circular dichroism spectra in protein stability studies. This material is available free of charge via the Internet at http://pubs.acs.org.

AUTHOR INFORMATION

Corresponding Author

*Department of Chemistry, Boston University, 590 Commonwealth Ave., Boston, MA 02215. Telephone: (617) 358-2816. Fax: (617) 353-6466. E-mail: elliott@bu.edu.

Funding

This work has been kindly supported by National Institutes of Health Grant R01 GM072663 to S.J.E. and National Science Foundation Grants CHE 0840418 and 1126545, and MCB 1122977.

Notes

The authors declare no competing financial interest.

ABBREVIATIONS

CAPS, *N*-cyclohexyl-3-aminopropanesulfonic acid; CD, circular dichroism; CHES, 2-(cyclohexylamino)ethanesulfonic acid; DNase I, deoxyribonuclease I; DTT, dithiothreitol; EPR, electron paramagnetic resonance; ER, endoplasmic reticulum; FPLC, fast protein liquid chromatography; IPTG, isopropyl β-D-1-thiogalactopyranoside; OMM, outer mitochondrial membrane; PBS, phosphate-buffered saline; MES, 2-(*N*-morpholino)ethanesulfonic acid; MOPS, 3-(*N*-morpholino)-propanesulfonic acid; PCET, proton-coupled electron transfer; PFV, protein film voltammetry; PMSF, phenylmethanesulfonyl fluoride; TAPS, 3-{[1,3-dihydroxy-2-(hydroxymethyl)propan-2-yl]amino}propane-1-sulfonic acid; TZD, thiazolidinedione.

REFERENCES

(1) Paddock, M. L., Wiley, S. E., Axelrod, H. L., Cohen, A. E., Roy, M., Abresch, E. C., Capraro, D., Murphy, A. N., Nechushtai, R., and Dixon, J. E. (2007) MitoNEET is a uniquely folded 2Fe−2S outer mitochondrial membrane protein stabilized by pioglitazone. *Proc. Natl. Acad. Sci. U.S.A. 104*, 14342−14347.

(2) Colca, J. R., McDonald, W. G., Waldon, D. J., Leone, J. W., Lull, J. M., Bannow, C. A., Lund, E. T., and Mathews, W. R. (2004) Identification of a novel mitochondrial protein ("mitoNEET") cross-linked specifically by a thiazolidinedione photoprobe. *Am. J. Physiol. 286*, E252−E260.

(3) Lin, J., Zhou, T., Ye, K., and Wang, J. (2007) Crystal structure of human mitoNEET reveals distinct groups of iron−sulfur proteins. *Proc. Natl. Acad. Sci. U.S.A. 104*, 14640−14645.

(4) Hou, X., Liu, R., Ross, S., Smart, E. J., Zhu, H., and Gong, W. (2007) Crystallographic studies of human MitoNEET. *J. Biol. Chem. 282*, 33242−33246.

(5) Wiley, S. E., Murphy, A. N., Ross, S. A., Van Der Geer, P., and Dixon, J. E. (2007) MitoNEET is an iron-containing outer mitochondrial membrane protein that regulates oxidative capacity. *Proc. Natl. Acad. Sci. U.S.A. 104*, 5318−5323.

(6) Wiley, S. E., Rardin, M. J., and Dixon, J. E. (2009) Localization and function of the 2Fe-2S outer mitochondrial membrane mitoNEET protein. *Methods Enzymol. 456*, 233−246.

(7) Zuris, J. A., Harir, Y., Conlan, A. R., Shvartsman, M., Michaeli, D., Tamir, S., Paddock, M. L., Onuchic, J. N., Mittler, R., Cabantchik, Z. I., Jennings, P. A., and Nechustai, R. (2011) Facile transfer of [2Fe-2S] clusters from the diabetes drug target mitoNEET to an apo-acceptor protein. *Proc. Natl. Acad. Sci. U.S.A. 108*, 13047−13052.

(8) Kusminski, C. M., Holland, W. L., Sun, K., Park, J., Spurgin, S. B., Lin, Y., Askew, G. R., Simcox, J. A., McClain, D. A., Li, C., and Scherer, P. E. (2012) MitoNEET-driven alterations in adipocyte mitochondrial activity reveal a crucial adaptive process that preserves insulin sensitivity in obesity. *Nat. Med. 18*, 1539−1549.

(9) Zhou, T., Lin, J., Feng, Y., and Wang, J. (2010) Binding of NADPH destabilizes the iron-sulfur clusters of human mitoNEET. *Biochemistry 49* (44), 9604−9612.

(10) Tsai, T. F., Chen, Y. F., and Tsai, S. F. (2009) CISD2-knockout mice and uses thereof. U.S. Patent Appl 12/481.

(11) Maiuri, M. C., Criollo, A., and Kroemer, G. (2010) Crosstalk between apoptosis and autophagy within the Beclin 1 interactome. *EMBO J. 29*, 515−516.

(12) Chen, Y. F., Wu, C. Y., Kirby, R., Kao, C. H., and Tsai, T. F. (2010) A role for the CISD2 gene in lifespan control and human disease. *Ann. N.Y. Acad. Sci. 1201*, 58−64.

(13) Chang, N. C., Nguyen, M., Germain, M., and Shore, G. C. (2009) Antagonism of Beclin 1-dependent autophagy by BCL-2 at the endoplasmic reticulum requires NAF-1. *EMBO J. 29*, 606−618.

(14) Bak, D. W., Zuris, J. A., Paddock, M. L., Jennings, P. A., and Elliott, S. J. (2009) Redox characterization of the FeS protein MitoNEET and impact of thiazolidinedione drug binding. *Biochemistry 48*, 10193−10195.

(15) Wiley, S. E., Paddock, M. L., Abresch, E. C., Gross, L., van der Geer, P., Nechushtai, R., Murphy, A. N., Jennings, P. A., and Dixon, J. E. (2007) The outer mitochondrial membrane protein mitoNEET contains a novel redox-active 2Fe-2S cluster. *J. Biol. Chem. 282*, 23745−23749.

(16) Iwasaki, T., Samoilova, R. I., Kounosu, A., Ohmori, D., and Dikanov, S. A. (2009) Continuous-wave and pulsed EPR characterization of the $[2Fe-2S](Cys)_3(His)_1$ cluster in rat mitoNEET. *J. Am. Chem. Soc. 131*, 13659−13667.

(17) Dicus, M. M., Conlan, A., Nechushtai, R., Jennings, P. A., Paddock, M. L., Britt, R. D., and Stoll, S. (2010) Binding of histidine in the $(Cys)_3(His)_1$-coordinated [2Fe−2S] cluster of human mitoNEET. *J. Am. Chem. Soc. 132*, 2037−2049.

(18) Fourmond, V., Hoke, K., Heering, H. A., Baffert, C., Leroux, F., Bertrand, P., and Léger, C. (2009) SOAS: A free program to analyze electrochemical data and other one-dimensional signals. *Bioelectrochemistry 76*, 141−147.
(19) Clark, W. M., and Clark, W. M. (1960) *Oxidation-reduction potentials of organic systems*, The Williams & Wilkins Co., Baltimore.
(20) Coghlan, V. M., and Vickery, L. E. (1991) Site-specific mutations in human ferredoxin that affect binding to ferredoxin reductase and cytochrome P450scc. *J. Biol. Chem. 266*, 18606−18612.
(21) Nechushtai, R., Conlan, A. R., Harir, Y., Song, L., Yogev, O., Eisenberg-Domovich, Y., Livnah, O., Michaeli, D., Rosen, R., Ma, V., Luo, Y., Zuris, J. A., Paddock, M. L., Cavantchil, Z. I., and Jennings , P. A. (2012) Characterization of *Arabidopsis* NEET reveals an ancient role for NEET proteins in iron metabolism. *Plant Cell 24* (5), 2139−2154.
(22) Léger, C., Elliott, S. J., Hoke, K. R., Jeuken, L. J. C., Jones, A. K., and Armstrong, F. A. (2003) Enzyme electrokinetics: Using protein film voltammetry to investigate redox enzymes and their mechanisms. *Biochemistry 42*, 8653−8662.
(23) Armstrong, F. (1990) Probing metalloproteins by voltammetry. *Bioinorg. Chem.*, 137−221.
(24) Armstrong, F. A., Heering, H. A., and Hirst, J. (1997) Reaction of complex metalloproteins studied by protein-film voltammetry. *Chem. Soc. Rev. 26*, 169−179.
(25) Zu, Y., Fee, J. A., and Hirst, J. (2001) Complete thermodynamic characterization of reduction and protonation of the bc 1-type Rieske [2Fe-2S] center of *Thermus thermophilus*. *J. Am. Chem. Soc. 123*, 9906−9907.
(26) Zu, Y., Manon, M. J. C., Kolling, D. R. J., Antony, R., Eltis, L. D., Fee, J. A., and Hirst, J. (2003) Reduction potentials of Rieske clusters: Importance of the coupling between oxidation state and histidine protonation state. *Biochemistry 42*, 12400−12408.
(27) Zuris, J. A., Halim, D. A., Conlan, A. R., Abresch, E. C., Nechushtai, R., Paddock, M. L., and Jennings, P. A. (2010) Engineering the redox potential over a wide range within a new class of FeS proteins. *J. Am. Chem. Soc. 132* (38), 13120−13122.
(28) Noodleman, L., Norman, J. G., Jr., Osborne, J. H., Aizman, A., and Case, D. A. (1985) Models for ferredoxins: Electronic structures of iron-sulfur clusters with one, two, and four iron atoms. *J. Am. Chem. Soc. 107*, 3418−3426.
(29) Lin, S. W., and Sakmar, T. P. (1996) Specific tryptophan UV-absorbance changes are probes of the transition of rhodopsin to its active state. *Biochemistry 35*, 11149−11159.
(30) Johnson, W. C. J. (1988) Secondary structure of proteins through circular dichroism spectroscopy. *Annu. Rev. Biophys. Biophys. Chem. 17*, 145−166.
(31) Leal, S. S., and Gomes, C. M. (2007) Studies of the molten globule state of ferredoxin: Structural characterization and implications on protein folding and iron-sulfur center assembly. *Proteins 68*, 606−616.
(32) Conlan, A. R., Axelrod, H. L., Cohen, A. E., Abresch, E. C., Zuris, J., Yee, D., Nechushtai, R., Jennings, P. A., and Paddock, M. L. (2009) Crystal structure of Miner1: The redox-active 2Fe-2S protein causative in Wolfram Syndrome 2. *J. Mol. Biol. 392*, 143−153.
(33) Lin, J., Zhang, L., Lai, S., and Ye, K. (2011) Structure and molecular evolution of CDGSH iron-sulfur domains. *PLoS One 6*, e24790.
(34) Hunsicker-Wang, L. M., Heine, A., Chen, Y., Luna, E. P., Todaro, T., Zhang, Y. M., Williams, P. A., McRee, D. E., Hirst, J., Stout, C. D., and Fee, J. A. (2003) High-resolution structure of the soluble, respiratory-type Rieske protein from *Thermus thermophilus*: Analysis and comparison. *Biochemistry 42*, 7303−7317.
(35) Camba, R., Jung, Y. S., Hunsicker-Wang, L. M., Burgess, B. K., Stout, C. D., Hirst, J., and Armstrong, F. A. (2003) Mechanisms of redox-coupled proton transfer in proteins: Role of the proximal proline in reactions of the [3Fe-4S] cluster in *Azotobacter vinelandii* ferredoxin I. *Biochemistry 42*, 10589−10599.
(36) Hu, J., Dong, L., and Outten, C. E. (2008) The redox environment in the mitochondrial intermembrane space is maintained separately from the cytosol and matrix. *J. Biol. Chem. 283*, 29126−29134.
(37) Hansen, J. M., Go, Y. M., and Jones, D. P. (2006) Nuclear and mitochondrial compartmentation of oxidative stress and redox signaling. *Annu. Rev. Pharmacol. Toxicol. 46*, 215−234.
(38) Schröter, T., Hatzfeld, O. M., Gemeinhardt, S., Korn, M., Friedrich, T., Ludwig, B., and Link, T. A. (1998) Mutational analysis of residues forming hydrogen bonds in the Rieske [2Fe-2S] cluster of the cytochrome bc1 complex in *Paracoccus denitrificans*. *Eur. J. Biochem. 255*, 100−106.
(39) Kim, J. H., Fuzery, A. K., Tonelli, M., Ta, D. T., Westler, W. M., Vickery, L. E., and Markley, J. L. (2009) Structure and dynamics of the iron-sulfur cluster assembly scaffold protein IscU and its interaction with the cochaperone HscB. *Biochemistry 48*, 6062−6071.
(40) Kim, J. H., Tonelli, M., and Markley, J. L. (2012) Disordered form of the scaffold protein IscU is the substrate for iron-sulfur cluster assembly on cysteine desulfurase. *Proc. Natl. Acad. Sci. U.S.A. 109*, 454−459.
(41) Adinolfi, S., Rizzo, F., Masino, L., Nair, M., Martin, S. R., Pastore, A., and Temussi, P. A. (2004) Bacterial IscU is a well folded and functional single domain protein. *Eur. J. Biochem. 271*, 2093−2100.
(42) Bertini, I., Cowan, J. A., Del Bianco, C., Luchinat, C., and Mansy, S. S. (2003) *Thermotoga maritima* IscU. Structural characterization and dynamics of a new class of metallochaperone. *J. Mol. Biol. 331*, 907−924.
(43) Mansy, S. S., Wu, G., Surerus, K. K., and Cowan, J. A. (2002) Iron-sulfur cluster biosynthesis. *Thermatoga maritima* IscU is a structured iron-sulfur cluster assembly protein. *J. Biol. Chem. 277*, 21397−21404.
(44) Mansy, S. S., Wu, S. P., and Cowan, J. A. (2004) Iron-sulfur cluster biosynthesis: Biochemical characterization of the conformational dynamics of *Thermotoga maritima* IscU and the relevance for cellular cluster assembly. *J. Biol. Chem. 279*, 10469−10475.
(45) Fleischhacker, A. S., Stubna, A., Hsueh, K. L., Guo, Y., Teter, S. J., Rose, J. C., Brunold, T. C., Markley, J. L., Münck, E., and Kiley, P. J. (2012) Characterization of the [2Fe-2S] cluster of *Escherichia coli* transcription factor IscR. *Biochemistry 51* (22), 4453−4462.
(46) Li, H., Mapolelo, D. T., Dingra, N. N., Naik, S. G., Lees, N. S., Hoffman, B. M., Riggs-Gelasco, P. J., Huynh, B. H., Johnson, M. K., and Outten, C. E. (2009) The yeast iron regulatory proteins Grx3/4 and Fra2 form heterodimeric complexes containing a [2Fe-2S] cluster with cysteinyl and histidyl ligation. *Biochemistry 48*, 9569−9581.
(47) Li, H., Mapolelo, D. T., Randeniya, S., Johnson, M. K., and Outten, C. E. (2012) Human glutaredoxin 3 forms [2Fe-2S]-bridged complexes with human BolA2. *Biochemistry 51* (8), 1687−1696.
(48) Giel, J. L., Rodionov, D., Liu, M., Blattner, F. R., and Kiley, P. J. (2006) IscR-dependent gene expression links iron-sulphur cluster assembly to the control of O_2-regulated genes in *Escherichia coli*. *Mol. Microbiol. 60*, 1058−1075.
(49) Li, H., and Outten, C. E. (2012) Monothiol CGFS glutaredoxins and BolA-like proteins: [2Fe-2S] binding partners in iron homeostasis. *Biochemistry 51* (22), 4377−4389.